JACS JOURNAL OF THE AMERICAN CHEMICAL SOCIETY

Communication

Cite This: *J. Am. Chem. Soc.* XXXX, XXX, XXX−XXX

pubs.acs.org/JACS

# Outer-Sphere Control of Catalysis on Surfaces: A Comparative Study of Ti(IV) Single-Sites Grafted on Amorphous versus Crystalline Silicates for Alkene Epoxidation

Nicolás A. Grosso-Giordano,[§] Christian Schroeder,[#] Alexander Okrut,[§] Andrew Solovyov,[§] Christian Schöttle,[§] Walter Chassé,[#] Nebojša Marinković,[‡] Hubert Koller,[*,#] Stacey I. Zones,[*,⊥] and Alexander Katz[*,§]

[§]Department of Chemical and Biomolecular Engineering, University of California, Berkeley, Berkeley, California 94720, United States
[#]Institut für Physikalische Chemie, Westfälische Wilhelms-Universität Münster, Münster 48149, Germany
[⊥]Chevron Energy Technology Company, Richmond, California 94804, United States
[‡]Department of Chemical Engineering, Columbia University, New York, New York 10027, United States

Ⓢ *Supporting Information*

**ABSTRACT:** The effect of outer-sphere environment on alkene epoxidation catalysis using an organic hydroperoxide oxidant is demonstrated for calix[4]arene-$Ti^{IV}$ single-sites grafted on amorphous vs crystalline delaminated zeotype (UCB-4) silicates as supports. A chelating calix[4]arene macrocyclic ligand helps enforce a constant $Ti^{IV}$ inner-sphere, as characterized by UV−visible and X-ray absorption spectroscopies, thus enabling the rigorous comparison of outer-sphere environments across different siliceous supports. These outer-sphere environments are characterized by solid-state $^1H$ NMR spectroscopy to comprise proximally organized silanols confined within 12 membered-ring cups in crystalline UCB-4, and are responsible for up to 5-fold enhancements in rates of epoxidation by $Ti^{IV}$ centers.

Supported catalytic active sites comprising isolated cations are ubiquitous;[1,2] however, their rational molecular design is currently hampered by a lack of understanding of how outer-sphere effects control their reactivity. Outer-sphere effects are controlled by surface moieties that are vicinal (noncoordinating) to the active centers,[3,4] as opposed to coordinating ligands of the inner-sphere,[5−9] and are commonly invoked in the reactivity of soluble molecular catalysts[10] and metalloenzymes.[11] Their experimental observation on supported molecular catalysts has been elusive, however, because of the challenges associated with modifying the outer-sphere without significantly affecting other aspects, such as inner-sphere or steric accessibility, of the active site.[12−18] Here, we demonstrate that outer-sphere environments have profound consequences on the reactivity of $Ti^{IV}$ sites supported on siliceous surfaces, the same type of active sites used in industrial propylene epoxidation catalysts.[19−21] Our approach enforces a constant inner-sphere environment for grafted $Ti^{IV}$ single-sites with a chelating macrocyclic calix[4]arene ligand, while maintaining active-site accessibility across crystalline zeolitic versus amorphous silicate outer-sphere environments of identical composition. This enables us to unequivocally determine that outer-sphere effects are responsible for rate enhancements of up to 5-fold per-$Ti^{IV}$-site in crystalline zeolitic supports during the catalytic epoxidation of cyclohexene with *t*-butyl hydroperoxide. NMR characterization reveals that these effects arise from differences in the proximal organization of surface silanol groups and their framework location relative to $Ti^{IV}$ active centers, demonstrating the importance of precisely designing outer-sphere structures for active sites on surfaces.

Our approach is shown in Scheme 1, and is based on a calix[4]arene-$Ti^{IV}$ surface complex (highlighted in brown) as a Lewis-acid catalytic $Ti^{IV}$ center. This is grafted onto a silanol (Si−OH) group on the surface of three different siliceous

**Scheme 1. Grafted Calix[4]arene-$Ti^{IV}$ Materials[a]**

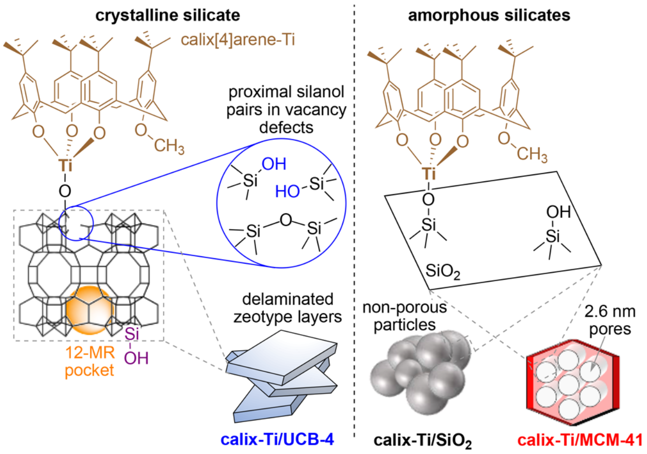

[a]Schematic representation of grafted calix[4]arene-$Ti^{IV}$ structures (brown). Details of the crystalline SSZ-70 (MWW-type) zeotype framework of UCB-4 (left panel) are shown along the a−c plane, with vertices representing $SiO_{4/2}$ tetrahedra connected by Si−O−Si bonds. Silanol (Si−OH) species characterized by NMR on SSZ-70 are represented as a proximal silanol pair in blue, and a crystal-terminating isolated silanol in purple.

**Received:** October 27, 2017
**Published:** March 22, 2018

DOI: 10.1021/jacs.7b11467

supports, consisting of a crystalline delaminated zeotype UCB-4 ,[22] and two amorphous silicas, which comprise Aerosil 200 fumed silica particles (denoted $SiO_2$) and MCM-41,[23] a hexagonally ordered silicate with uniform 2.6 nm mesopores (Supporting Information 1 and 2).[24] The resulting catalysts comprising grafted calix[4]arene-$Ti^{IV}$ complexes are denoted calix-Ti/SUP, where SUP = UCB-4, $SiO_2$, or MCM-41 indicates the support in Scheme 1, with physicochemical properties summarized in Table 1. Upon grafting, calix[4]arene-to-Ti ratios in all catalysts were measured to be near unity (calix:Ti in Table 1), confirming that the surface complex is intact and that the calix[4]arene ligand remains bound to $Ti^{IV}$,[25] as depicted in Scheme 1. The macrocyclic dimensions of the calix[4]arene-$Ti^{IV}$ precursor prevent its diffusion into zeotype micropores during grafting, ensuring that grafting occurs on the external surface only, as also indicated by analysis of grafting densities (Supporting Information 3). The location of all active sites on the external surface ensures their equal accessibility for activation of organic hydroperoxides in the absence of steric limitations imposed by zeolitic micropores,[26,27] enabling a direct and rigorous comparison of intrinsic calix[4]arene-$Ti^{IV}$ reactivity across all materials.

**Table 1. Physicochemical Properties of Supports and $Ti^{IV}$-Containing Materials**

| Support | wt % Ti | Calix:Ti | LMCT edge (eV) | $A_{rel}$[a] | $k_{eff}$[b] |
|---|---|---|---|---|---|
| $SiO_2$ | 0.35 | 1.0 | 2.29 | 0.92 | 8 |
| MCM-41 | 0.70 | 1.0 | 2.21 | 0.89 | 10 |
| UCB-4 | 0.37 | 1.1 | 2.24 | 0.93 | 42 |

[a] Ratio of Ti K-edge XANES pre-edge area features, ±0.07 (Supporting Information 1.3 and 6). [b] Effective epoxidation rate constant, $M^{-2}$ $s^{-1}$, ±1 (Supporting Information 1.4 and 7).

The outer-sphere environment as controlled by the support surface surrounding the grafted calix[4]arene-$Ti^{IV}$ complex is compositionally identical in all siliceous supports. However, it contrasts in (i) the ordered crystalline versus random amorphous arrangement of the silicate framework, and (ii) the organization of surface silanols (Si−OH) onto which calix[4]arene-$Ti^{IV}$ complexes are grafted.[28] This is respectively illustrated by (i) the presence of 12 membered-ring pockets (12-MR pocket in Scheme 1) on the external surface of crystalline UCB-4,[29] which are absent in amorphous $SiO_2$ and MCM-41;[24] and (ii) the random distribution of isolated silanol groups on the surface of these partially dehydroxylated amorphous silicates, in contrast to silanol organization into cooperative proximal arrangements in crystalline UCB-4 (Scheme 1).[28] These arrangements are synthesized by the postsynthetic hydrolysis and removal of $B^{III}$ from rigid zeolitic frameworks such as SSZ-70 studied here, exposing a vacancy defect terminated by silanols (vide infra).

Given the role that silanol groups have on the grafting and outer-sphere environments of calix[4]arene-$Ti^{IV}$ sites, we investigated their nature and local organization in both crystalline and amorphous supports by solid-state $^1H$ NMR spectroscopy, prior to calix[4]arene-$Ti^{IV}$ grafting (in order to reduce interference of $^1H$ signals from organics). We chose to examine the nondelaminated B-SSZ-70, the calcined variant of the layered zeotype precursor that leads to UCB-4 (Supporting Information 1.1 and 2), because delamination does not affect calix[4]arene-$Ti^{IV}$ grafting densities or per-$Ti^{IV}$-site catalytic activity (Table S2 and Figure S5). After $B^{III}$ removal from the borosilicate framework of B-SSZ-70, there is an appearance of resonances corresponding to silanols in the $^1H$ MAS NMR spectrum at 2−8 ppm (Figure S2A). The $^1H$ single-quantum double-quantum (SQ-DQ) MAS NMR dipolar correlation spectrum shows two well-resolved cross-correlation peaks (Figure 1A) for hydrogen-bonded silanols, at 3.3 and 4.0 ppm. This cross-correlation rigorously confirms two silanols comprising different chemical shifts to be adjacent in space, indicative of a well-ordered paired silanol arrangement being formed in vacancies exposed by $B^{III}$ removal, as depicted in blue in Scheme 1. Corresponding data for B-SSZ-70 where $B^{III}$ remains part of the crystalline framework (Figure S2Ca) confirms that this arrangement does not exist prior to $B^{III}$ removal. Such deboronation treatments are generally believed to synthesize vacancy defect structures termed "silanol nests" in zeotype frameworks, consisting of four hydrogen-bonded

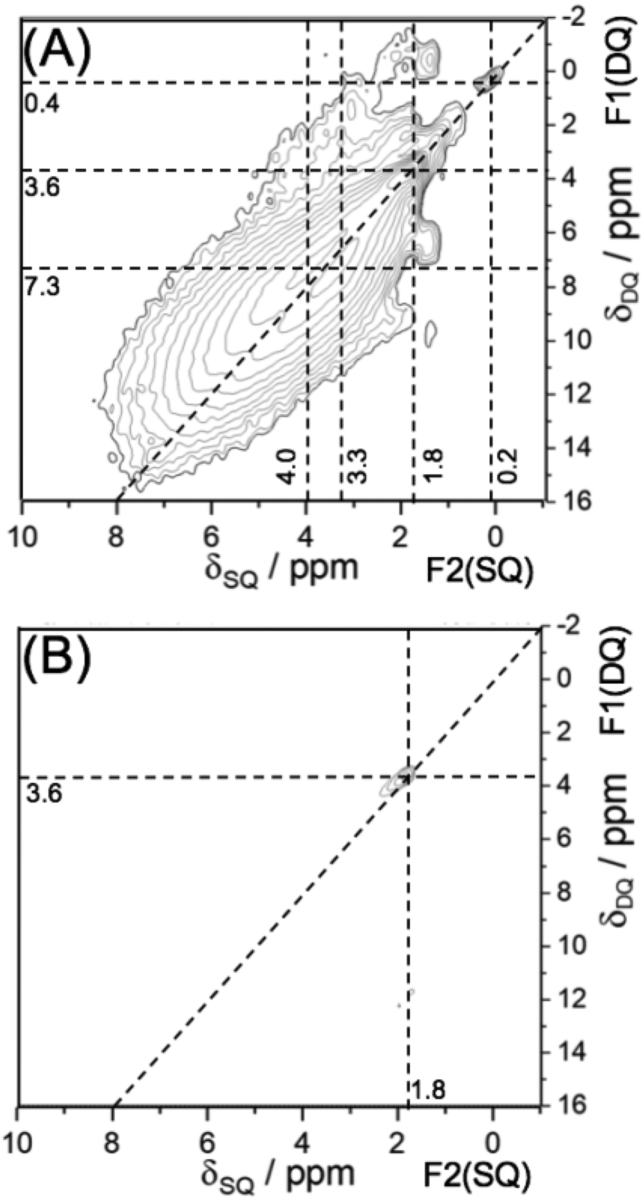

**Figure 1.** $^1H$ SQ DQ MAS NMR spectra acquired at a magnetic field strength of 9.74 T and a MAS rate of 9000 Hz of (A) B-SSZ-70 after $B^{III}$ removal, and (B) $SiO_2$.

silanols; however, no rigorous study has determined the actual number of silanols involved in such structures.[30] Our 2Q NMR data unequivocally demonstrates the existence of at least two such paired silanols in SSZ-70, and all attempts by $^1$H NMR to show the presence of more than two silanols employing 3Q or 4Q excitation have been unsuccessful. In contrast, the amorphous $SiO_2$ support (dehydroxylated at 823 K) shows no signal for hydrogen-bonded silanols, and its SQ-DQ MAS NMR spectrum shows only a weak autocorrelation signal at 1.8 ppm (Figure 1B), corresponding to randomly paired surface silanols, whose abundance is insignificant when compared to the paired silanols in SSZ-70 (Supporting Information 4).

In order to quantify the pairing and distances between silanol groups, $^1$H DQ build-up curves were measured.[31] These data on SSZ-70 reveal that 34% of silanols are found within well-ordered pairs, with a $^1$H−$^1$H distance of 2.5 Å (Figure S2Db and Supporting Information 4). This distance indicates that considerable rearrangement of the local structure is necessary upon $B^{III}$ removal, as the average edge length (between oxygen atoms) of a tetrahedral center is 2.6 Å. A minority of silanols in SSZ-70 are isolated species on its external crystal-terminating surface, with signal at 1.8 ppm,[32] depicted in purple in Scheme 1. In amorphous $SiO_2$, the vast majority (82%) of silanols are isolated, while the remaining protons exhibit an instant rise to maximum double-quantum intensity at early evolution times (Figure S2Da), with an extremely large dipolar coupling constant of at least 15 kHz (indicating a H−H distance below 2.0 Å), unlikely to represent paired silanols and instead typical of rigidly adsorbed water (H−H distance of 1.6 Å).

Because of the close proximity of silanol pairs in UCB-4, multidentate support Si−O−$Ti^{IV}$ connectivity is possible in principle, at the expense of breaking some Ti−O(calix) bonds. To address this, we measured calix[4]arene-$Ti^{IV}$ ligand-to-metal charge-transfer (LMCT) edge-energies for calix-Ti/SUP materials, since this energy has been previously reported to be sensitive to the number of covalent connections between calix[4]arene oxygens and grafted $Ti^{IV}$ cations.[33] These values are all measured to be 2.25 ± 0.05 eV (Table 1), consistent with tridentate calix[4]arene connectivity and single-point attachment to support, as two-point attachment of the calix[4]arene would have resulted in a lower edge energy of 2.14 eV (see Supporting Information 5).[33] This confirms the equivalent inner-sphere coordination for $Ti^{IV}$ in all catalysts, as depicted in Scheme 1.

To investigate possible variations in electronic environment of $Ti^{IV}$ centers grafted on different supports, we performed Ti K-edge XANES,[34,35] with results shown in Figure 2. Pre-edge features, highlighted in the inset of Figure 2, arise from electronic transitions of core electrons into empty 3d orbitals of $d^0$ $Ti^{IV}$, and are thus a descriptor of 3d orbital availability and Lewis-acid strength.[35] This descriptor is quantified by the value of $A_{rel}$ in Table 1 (Supporting Information 1.3 and 6), and its value of 0.9 together with pre-edge positions at 4970 eV is consistent with site-isolated 4-coordinate $Ti^{IV}$ centers within grafted calix[4]arene-$Ti^{IV}$ surface complexes.[3,35,36] The lack of changes in these values and pre-edge peak heights across all materials (Figure 2 and Table 1), within experimental uncertainty, confirms the identical 3d orbital occupancy and inner-sphere of $Ti^{IV}$ centers across all catalysts.

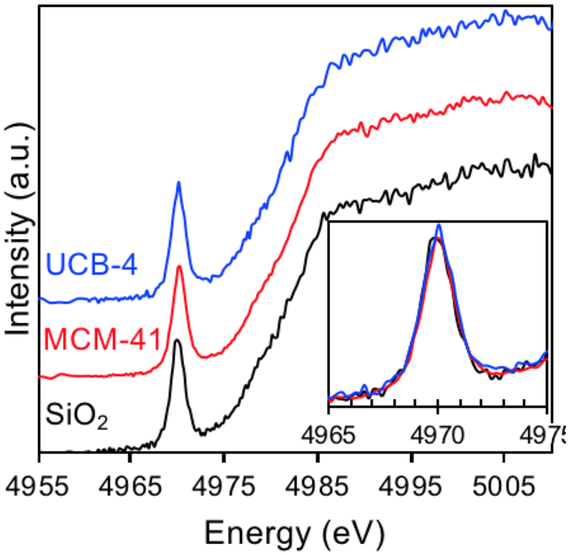

**Figure 2.** Normalized Ti K-edge XANES spectra, with inset detailing the pre-edge region, for calix[4]arene-$Ti^{IV}$ sites on the labeled support.

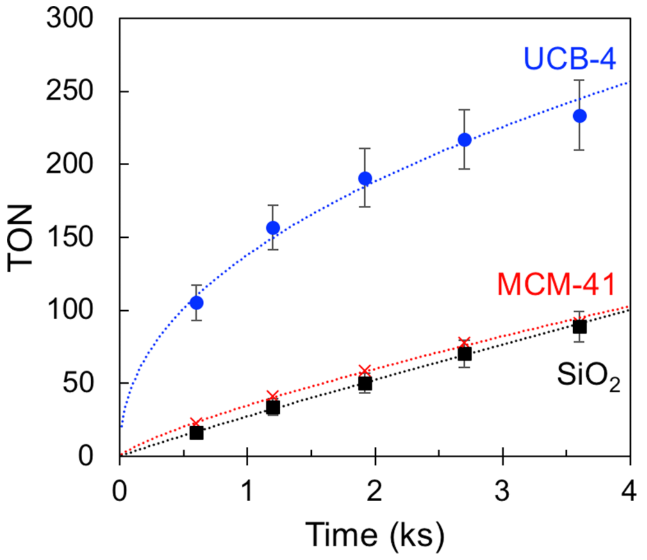

**Figure 3.** Catalytic turnover numbers (TON) for epoxide production as a function of time, for calix[4]arene-$Ti^{IV}$ sites on the labeled support.

Rate constants normalized by $Ti^{IV}$ contents ($k_{eff}$) for the epoxidation of cyclohexene with *tert*-butyl hydroperoxide (Scheme S3), a common probe reaction for epoxidation activity, are summarized in Table 1 for all calix-Ti/SUP catalysts, with epoxide yields uniformly high (Figure S6B). Values of $k_{eff}$ are observed to be 4- and 5-fold higher in crystalline calix-Ti/UCB-4, as compared to amorphous calix-Ti/MCM-41 and calix-Ti/$SiO_2$, respectively. Similar enhancements favoring calix-Ti/UCB-4 are also observed when quantifying turnover numbers for epoxide production (Figure 3), irrespective of whether the amorphous support contains a well-ordered porous system in MCM-41 or not ($SiO_2$). We surmise that, on a single-site basis, all $Ti^{IV}$ centers behave similarly when grafted on amorphous supports, as described previously,[26] but with distinctly lower activity than on crystalline calix-Ti/UCB-4. Control experiments were performed to confirm that the high-activity in calix-Ti/UCB-4 relative to the amorphous catalysts is not due to artifacts of delamination, acid washing treatment, presence of $B^{III}$, or diffusional constraints, is independent of calix[4]arene-$Ti^{IV}$

surface density (Supporting Information 3), and is generalizable to other olefins and oxidants (Supporting Information 7). Significantly, calix[4]arene-$Ti^{IV}$ sites grafted on fully hydroxylated $SiO_2$ (calix-Ti/$SiO_2$-AW in Supporting Information 3) exhibit rates equivalent to those of calix-Ti/$SiO_2$ ($k_{eff}$ = 8 $M^{-2}$ $s^{-1}$), indicating that silanol pairing as achieved by high local silanol densities on amorphous silicates is alone insufficient for enhancing reactivity.

Based on the identical electronic and inner-sphere environments of grafted $Ti^{IV}$ for all catalysts, active sites would be expected to display similar epoxidation rates in the absence of outer-sphere effects; however, they are instead observed to be up to 5-fold more active when grafted on the crystalline framework of UCB-4, in comparison to amorphous supports. We conclude that these enhancements in rate are brought about by outer-sphere effects intrinsic to the support in calix-Ti/UCB-4. These effects specifically involve paired silanols located within 12-MR pockets in UCB-4, distinct from those present in fully hydroxylated amorphous $SiO_2$, where surface heterogeneity precludes a precise location of silanol pairs with respect to active centers. Calix[4]arene-$Ti^{IV}$ grafting on UCB-4 may occur on one of the two silanols in the organized pair, thereby leaving one silanol in close proximity to the $Ti^{IV}$ site, or on the exterior surface, adjacent to the silanol pair. In either scenario, the existence of a neighboring silanol may facilitate the activation of bound intermediates (e.g., for hydroperoxide binding or subsequent transfer of oxygen to epoxide),[37,38] giving rise to the observed outer-sphere effects. While these effects have long been hypothesized,[39] challenges in controlling $Ti^{IV}$ inner-spheres[40] and steric accessibility across supports have precluded their observation,[26,27] despite decades of seminal work.[41,42] Our synthetic approach overcomes these challenges, providing the first rigorous experimental demonstration of outer-sphere effects on per-site activity in titanosilicates.

Our findings evidence the role of organization and location of outer-sphere functionalities for catalysis on surfaces, analogous to outer-sphere residue cooperativity within active sites of certain protease enzymes.[43] By exploiting delaminated zeotypes as accessible crystalline supports with well-defined surface environments, optimal active sites that incorporate outer-sphere functionalities can be rationally designed. Such approaches may lead to improvements in olefin epoxidation catalysts,[44,45] where state-of-the-art technologies still rely on amorphous supports when using organic hydroperoxides as oxidants,[19−21] and in catalysis on surfaces in general, where control over the strucutral environment comprising functional groups surrounding active centers is only beginning to emerge.

## ■ ASSOCIATED CONTENT

### Ⓢ Supporting Information

The Supporting Information is available free of charge on the ACS Publications website at DOI: 10.1021/jacs.7b11467.

> Experimental methods, support textural properties, NMR characterization, analysis of LMCT edge-energies, testing of control materials, details of Ti K-edge XANES spectra, kinetic analysis, and supplementary references (PDF)

## ■ AUTHOR INFORMATION

### Corresponding Authors

*askatz@berkeley.edu
*sizo@chevron.com
*hubert.koller@uni-muenster.de

### ORCID

Nicolás A. Grosso-Giordano: 0000-0002-0912-366X
Christian Schöttle: 0000-0001-9537-1573
Walter Chassé: 0000-0002-6079-3415
Hubert Koller: 0000-0003-4029-8262
Alexander Katz: 0000-0003-3487-7049

### Notes

The authors declare the following competing financial interest(s): (1) The funding for the research partially came from Chevron Energy Technology Co. and (2) Stacey I. Zones is an employee and stockholder in Chevron Corp.

## ■ ACKNOWLEDGMENTS

Funding from the National Science Foundation (PFI:AIR-TT 2801542974), Office of Basic Energy Sciences of Department of Energy (DE-FG02-05ER15696) and the Deutsche Forschungsgemeinschaft (DFG, German Research Foundation, KO 1817/3-1) are gratefully acknowledged. The authors are grateful to the Management and Transfer of Hydrogen via Catalysis Program funded by Chevron Corporation. XAS measurements were performed on SSRL Beamline 2-2, which was supported in part by the Synchrotron Catalysis Consortium, U.S. Department of Energy Grant No. DE-SC0012335.

## ■ REFERENCES

(1) Pelletier, J. D. A.; Basset, J. M. *Acc. Chem. Res.* **2016**, *49*, 664.

(2) Thomas, J. M. *Design and applications of single-site heterogeneous catalysts: contributions to green chemistry, clean technology and sustainability*; Imperial College Press: London, 2012.

(3) Notestein, J. M.; Solovyov, A.; Andrini, L. R.; Requejo, F. G.; Katz, A.; Iglesia, E. *J. Am. Chem. Soc.* **2007**, *129*, 15585.

(4) Bass, J. D.; Anderson, S. L.; Katz, A. *Angew. Chem., Int. Ed.* **2003**, *42*, 5219.

(5) Bouh, A. O.; Rice, G. L.; Scott, S. L. *J. Am. Chem. Soc.* **1999**, *121*, 7201.

(6) Lu, J.; Aydin, C.; Liang, A. J.; Chen, C. Y.; Browning, N. D.; Gates, B. C. *ACS Catal.* **2012**, *2*, 1002.

(7) Nandi, P.; Tang, W.; Okrut, A.; Kong, X.; Hwang, S.-J.; Neurock, M.; Katz, A. *Proc. Natl. Acad. Sci. U. S. A.* **2013**, *110*, 2484.

(8) Bordiga, S.; Bonino, F.; Damin, A.; Lamberti, C. *Phys. Chem. Chem. Phys.* **2007**, *9*, 4854.

(9) Radhakrishnan, R.; Oyama, S. T.; Chen, J. G.; Asakura, K. *J. Phys. Chem. B* **2001**, *105*, 4245.

(10) Comas-Vives, A.; Ujaque, G.; Lledós, A. *Adv. Inorg. Chem.* **2010**, *62*, 231.

(11) Edwards, R. A.; Whittaker, M. M.; Whittaker, J. W.; Baker, E. N.; Jameson, G. B. *Biochemistry* **2001**, *40*, 15.

(12) Bermejo-Deval, R.; Orazov, M.; Gounder, R.; Hwang, S. J.; Davis, M. E. *ACS Catal.* **2014**, *4*, 2288.

(13) Comotti, M.; Li, W.-C.; Spliethoff, B.; Schüth, F. *J. Am. Chem. Soc.* **2006**, *128*, 917.

(14) Grosso-Giordano, N. A.; Eaton, T. R.; Bo, Z.; Yacob, S.; Yang, C. C.; Notestein, J. M. *Appl. Catal., B* **2016**, *192*, 93.

(15) Lu, J.; Serna, P.; Aydin, C.; Browning, N. D.; Gates, B. C. *J. Am. Chem. Soc.* **2011**, *133*, 16186.

(16) Liu, J.; Lucci, F. R.; Yang, M.; Lee, S.; Marcinkowski, M. D.; Therrien, A. J.; Williams, C. T.; Sykes, E. C. H.; Flytzani-Stephanopoulos, M. *J. Am. Chem. Soc.* **2016**, *138*, 6396.

(17) Park, J. W.; Thomas, K.; Van Gestel, J.; Gilson, J. P.; Collet, C.; Dath, J. P.; Houalla, M. *Appl. Catal., A* **2010**, *388*, 37.

(18) Dijkmans, J.; Dusselier, M.; Janssens, W.; Trekels, M.; Vantomme, A.; Breynaert, E.; Kirschhock, C.; Sels, B. F. *ACS Catal.* **2016**, *6*, 31.

(19) Oyama, S. T. *Mechanisms in Homogeneous and Heterogeneous Epoxidation Catalysis*; Elsevier: Amsterdam, 2011.
(20) Sheldon, R. A.; Van Doorn, J. A. *J. Catal.* **1973**, *31*, 427.
(21) Sheldon, R. A. *J. Mol. Catal.* **1980**, *7*, 107.
(22) Ogino, I.; Eilertsen, E. A.; Hwang, S.-J.; Rea, T.; Xie, D.; Ouyang, X.; Zones, S. I.; Katz, A. *Chem. Mater.* **2013**, *25*, 1502.
(23) Sever, R. R.; Alcala, R.; Dumesic, J. A.; Root, T. W. *Microporous Mesoporous Mater.* **2003**, *66*, 53.
(24) Chen, C.-Y.; Li, H.-X.; Davis, M. E. *Microporous Mater.* **1993**, *2*, 17.
(25) Notestein, J. M.; Iglesia, E.; Katz, A. *J. Am. Chem. Soc.* **2004**, *126*, 16478.
(26) Blasco, T.; Corma, A.; Navarro, M. T.; Pérez Pariente, J. *J. Catal.* **1995**, *156*, 65.
(27) Khouw, C.; Dartt, C. B.; Labinger, J. A.; Davis, M. E. *J. Catal.* **1994**, *149*, 195−205.
(28) Grosso-Giordano, N. A.; Yeh, A. J. Y. J.; Okrut, A.; Xiao, D. J.; Grandjean, F.; Long, G. J.; Zones, S. I.; Katz, A. *Chem. Mater.* **2017**, *29*, 6480.
(29) Hsieh, M.-F. Ph.D. Dissertation, University of California, Santa Barbara, CA, 2014.
(30) Senderov, E.; Halasz, I.; Olson, D. H. *Microporous Mesoporous Mater.* **2014**, *186*, 94.
(31) Chassé, W.; Valentín, J. L.; Genesky, G. D.; Cohen, C.; Saalwächter, K. *J. Chem. Phys.* **2011**, *134*, 044907.
(32) Shantz, D. F.; Schmedt Auf Der Günne, J.; Koller, H.; Lobo, R. F. *J. Am. Chem. Soc.* **2000**, *122*, 6659.
(33) Grosso-Giordano, N. A.; Solovyov, A.; Hwang, S.-J.; Katz, A. *Top. Catal.* **2016**, *59*, 1110.
(34) Thomas, J. M.; Sankar, G. *Acc. Chem. Res.* **2001**, *34*, 571.
(35) Notestein, J. M.; Andrini, L. R.; Kalchenko, V. I.; Requejo, F. G.; Katz, A.; Iglesia, E. *J. Am. Chem. Soc.* **2007**, *129*, 1122.
(36) Eaton, T. R.; Campos, M. P.; Gray, K. A.; Notestein, J. M. *J. Catal.* **2014**, *309*, 156.
(37) Khouw, C. B.; Davis, M. E. *J. Catal.* **1995**, *151*, 77.
(38) Wells, D. H.; Joshi, A. M.; Delgass, W. N.; Thomson, K. T. *J. Phys. Chem. B* **2006**, *110*, 14627.
(39) Wells, D. H.; Delgass, W. N.; Thomson, K. T. *J. Am. Chem. Soc.* **2004**, *126*, 2956.
(40) Eaton, T. R.; Boston, A. M.; Thompson, A. B.; Gray, K. A.; Notestein, J. M. *ChemCatChem* **2014**, *6*, 3215.
(41) Ratnasamy, P.; Srinivas, D.; Knözinger, H. *Adv. Catal.* **2004**, *48*, 1.
(42) See Supporting Information Section 8.
(43) Carter, P.; Wells, J. A. *Nature* **1988**, *332*, 564.
(44) Aigner, M.; Grosso-Giordano, N. A.; Schottle, C.; Okrut, A.; Zones, S.; Katz, A. *React. Chem. Eng.* **2017**, *2*, 852.
(45) Aigner, M.; Grosso-Giordano, N. A.; Okrut, A.; Zones, S. I.; Katz, A. *React. Chem. Eng.* **2017**, *2*, 842.

DOI: 10.1021/jacs.7b11467
*J. Am. Chem. Soc.* XXXX, XXX, XXX−XXX